A High Performance Enzyme-Free Glucose Sensor Based on the Graphene-CuO Nanocomposites

Yancai Li[1,2], Fuying Huang[1,2], Jie Chen[1], Tao Mo[1], Shunxing Li[1,2,], Fei Wang[1,2], Shuqing Feng[1,2], Yuanjun Li[1,2]*

[1] Department of Chemistry & Environmental Science, Zhangzhou Normal University, Zhangzhou 363000, PR China
[2] Fujian Province Key Laboratory of Modern Analytical Science and Separation Technology, Zhangzhou Normal University, Zhangzhou 363000, PR China
[*]E-mail: lishunxing@fjzs.edu.cn

Graphene-CuO nanocomposites were synthesized on a template of graphene by a one-step chemical synthesis approach and used to fabricate an enzyme-free amperometric glucose sensor. The fabricated glucose sensor showed that the linear dependence was from 2.0 μM to 0.06 mM, with high sensitivity of 1480 μA mM^{-1} cm^{-2}, fast response time of 3 s and low detection limit of 0.29 μM (*S/N*=3). Furthermore, the sensor is highly resistant against poisoning by chloride ion; the interference from the common interfering species such as ascorbic acid (AA), dopamine (DA), uric acid (UA) can be effectively avoided; the sensor also displayed long-term stability to glucose. These results indicate that the graphene-CuO nanocomposites are promising candidates for the non-enzymatic detection of glucose.

1. INTRODUCTION

Reliable and fast determination of glucose is essential in clinical diagnostics, biotechnology and the food industry [1-3]. Although glucose oxidase (GOx) has been widely used to construct various amperometric biosensors for the detection of glucose, enzymatic glucose biosensors suffer from the lack of stability due to the intrinsic nature of GOx. In recent years, considerable attention has been paid to developing a non-enzymatic glucose sensor to solve this problem. The direct electrocatalytic oxidation of glucose can be realized on electrodes modified with precious metals [4,5],

metal nanoparticles [6,7], and metal alloys [8,9], which exhibit an enhanced stability and activity. CuO, a p-type semiconductor with a narrow band gap of 1.2 eV, has been widely studied because of its extensive applications in catalysis, semiconductors, gas sensors, biosensors, and field transistors [10-13]. Some efforts are being made on amperometric determination of glucose using CuO nanomaterials [14,15].

Graphene, as a single layer of carbon atoms in a closely packed honeycomb two-dimensional lattice, has attracted a great deal of attentions since it was first reported in 2004 [16]. Compared with carbon nanotubes, graphene possesses larger specific surface area, higher purity, higher conductivity and lower cost, and could be regarded as unrolled carbon nanotubes [17]. Owing to the high conductivity and specific surface area, graphene-based materials have recently received increasing attentions in the field of electroanalysis [18,19]. To date, graphene-based electrochemical sensors have been used for the detection of DA, H_2O_2 and AA as well as other substances [20,21]. Considering the attractive properties of graphene, it is expected that graphene could provide an excellent support for the CuO nanoparticles to promote efficient electron transfer in the oxidation of glucose. However, to our best knowledge, there is little research on decorating CuO nanoparticles on graphene surface for non-enzymatic glucose detection.

In this paper, the graphene-CuO nanocomposites were synthesized by a one-step chemical synthesis approach. Combined with the advantages of graphene and CuO nanoparticles, we developed a novel enzyme-free glucose sensor by immobilizing the nanocomposites on glassy carbon electrode (GCE) with Nafion. The structure and morphology of the graphene-CuO nanocomposites were characterized by X-Ray Diffraction (XRD), transmission electron microscope (TEM) and Raman spectroscopy. The electrochemical performance of the graphene-CuO/Nafion/GCE for the detection of glucose was investigated by cyclic voltammetry (CV), electrochemical impendance spectrum (EIS) and amperometric I-t curve. The graphene-CuO/Nafion/GCE shows much better electrocatalytic properties for the glucose oxidation than the unmodified graphene sheets electrode or other non-enzymatic glucose sensors reported in the literature [10,14,15,21]. Moreover, the as-prepared electrode exhibits high sensitivity, excellent selectivity, fast response and good stability, which is promising to be an excellent non-enzymatic glucose sensor.

2. EXPERIMENTAL

2.1. Reagents and materials

Glucose and AA were obtained from Beijing Chemical Company (Beijing, China); GOx and UA were purchased from sangon biotech (shanghai, China) co. Ltd; DA and Nafion (5wt.%) were obtained from Sigma-Aldrich; The 0.02 M sodium hydroxide (NaOH) was employed as a supporting electrolyte. All other chemicals were of analytical grade and were used without further purification. All solutions were made up with double-distilled water.

2.2. Apparatus

TEM was performed on a FEI Tecnai G2 20 ST and HRTEM was performed on a FEI Tecnai G2 F20 electron microscope operated at 200 kV with the software package for automated electron tomography. Powder XRD patterns were recorded on a Panaltical X'Pert-pro MPD X-ray power diffractometer, using Cu Kα radiation. Raman spectra were recorded with a Jobin-Yvon LabRam HR800 confocal Raman spectrometer. All electrochemical measurements were performed at room temperature using a CHI 660D electrochemical workstation (Chenhua Instrument Co., Shanghai, China). A conventional three-electrode system was used with an Ag/AgCl (saturated KCl) electrode as the reference electrode, a platinum wire as the counter electrode, and a modified glassy carbon electrode (GCE, 3mm in diameter) as the working electrode.

2.3. Synthesis of graphene-CuO nanocomposites

The graphene nanosheet was synthesized from natural graphite using a modified Hummers method [22]. Graphene-CuO nanocomposites were synthesized by a modified Wang's method [23,24]. In a typical process, 2 mL (1.5 mg/mL) of aqueous dispersion graphene was dispersed in 15 mL of N,N-dimethylformamide (DMF). Then, 1.5 mL of 0.2 M cupric acetate aqueous solution was injected into the above solution with ultrasound for 2.5 hours. The resulting suspension was sealed in stainless steel autoclave tubes for reaction at 140 ℃ for 8 hours. The final products were collected by centrifugation, water-washed and dried. For comparison, the CuO nanoparticles were synthesized in the same way except for the addition of the aqueous dispersion graphene.

2.4. Preparation of the graphene-CuO/Nafion electrode

The modified electrode was prepared as follows: the GCE was polished with alumina slurry, and then ultrasonically cleaned alternately in ethanol and double-distilled water. Graphene-CuO nanocomposites (8mg) were dissolved in a mixture of 0.1 mL Nafion and 0.9 mL distilled water. A black suspension was obtained under ultrasonic agitation for a few minutes. Then 10μL of the mixture was dropped onto the cleaned GCE and allowed to dry at 4 ℃. The electrode was taken as the graphene-CuO/Nafion/GCE. A similar procedure was employed to fabricate the CuO/Nafion/GCE.

3. RESULTS AND DISCUSSION

3.1. Structural characterization

The morphology of the as-synthesized graphene, CuO nanoparticles and graphene-CuO nanocomposites were characterized by TEM, as shown in Fig. 1A, B and C. It can be seen that the graphene shows an ultrathin wrinkled paper-like structure and the CuO nanoparticles tend to aggregate into clusters with size of 20-100 nm. In the graphene-CuO nanocomposites, high-density nanograins of

CuO with uniform size of about 5 nm are distributed evenly throughout the graphene sheets. High-resolution transmission electron microscopy (HRTEM) enables the viewing of lattice planes, confirming crystallinity within the nanograins.
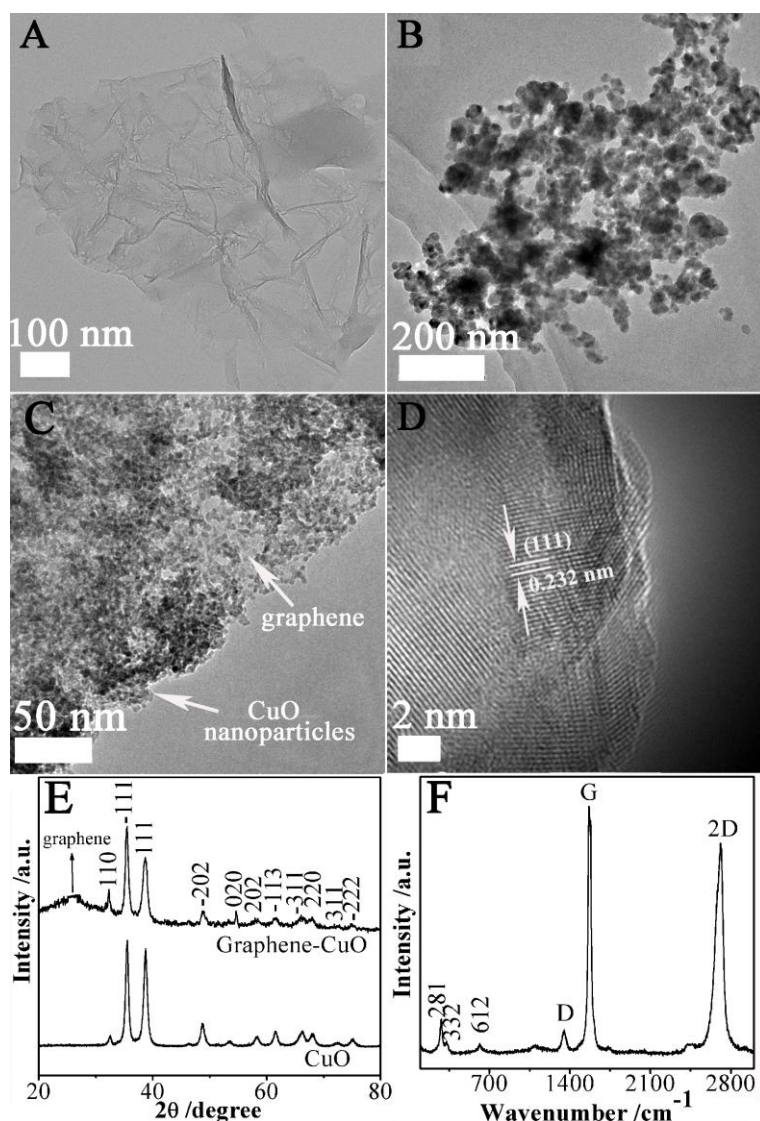
Figure 1. TEM images of (A) graphene, (B) CuO nanoparticles and (C) graphene-CuO nanocomposites; (D) HRTEM images of graphene-CuO nanocomposites; (E) XRD patterns of CuO nanoparticles and graphene-CuO nanocomposites; (F) Raman spectra of graphene-CuO nanocomposites.

The lattice spacing is about 0.232 nm between adjacent lattice planes of the CuO nanograins (Fig. 1D), which agrees well with the calculated value based on (111) planes of CuO. The uniform quantum size, good crystallinity and well-separated distribution of CuO nanograins on the graphene surface, can be ascribed to the usage of the favorable template of graphene and the one-step synthesis method. It is well known that graphene bears a closely packed honeycomb two-dimensional lattice of carbon atoms in a single layer. In the synthetic process, the reactants could be oriented to the carbon

atoms on graphene; at the reactive centers, CuO could be directly produced and undergo the growth along a certain direction into nanocrystals. Thus, the excellent template of graphene and the one-step synthesis could account for smaller size and better crystallinity of CuO nanograins in this case than in ref. [21].

XRD patterns of as-synthesized CuO nanoparticles and graphene-CuO nanocomposites are shown in Fig. 1E. All the peaks can be assigned to CuO and graphene, in which the CuO peaks are well indexed to a monoclinic symmetry (space group C2/c; a0=4.684Å, b0=3.425Å, c0=5.129Å, ß=99.47°, JCPDS Card No. 05 0661), and the graphene peak at 25° is attributed to the (002) plane of hexagonal graphite structure. In contrast, the graphene-CuO nanocomposites show broader peaks with lower intensity than the CuO nanoparticles, suggesting a smaller size of CuO nanograins in the nanocomposites.

Raman spectroscopy has historically played an important role in the structural characterization of graphitic materials [25,26]. A typical Raman spectrum of graphene-CuO nanocomposites is presented in Fig.1F. The ratio of the 2D peak (2700 cm^{-1}) to the G peak (1595 cm^{-1}) and a single G peak indicated the formation of double-layer graphene [27]. The presence of a very weak D band feature reveals defects produced in the nanocomposites preparation, but at a minimal level. The extra peaks at 281, 332 and 612 cm^{-1} should correspond to the one A_g and two B_g modes of vibrations of CuO, respectively [28].

3.2. Electrochemical characterization
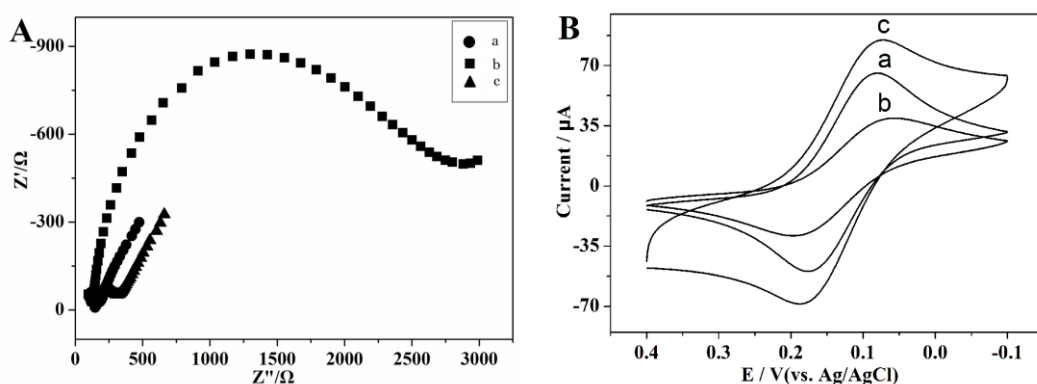
Figure 2. (A) EIS and (B) CVs of: (a) Bare GCE; (b) CuO/Nafion/GCE; (c) graphene-CuO/Nafion/GCE in 0.1 M KCl electrolyte solution containing 0.01 M Fe(CN)$_6^{4-/3-}$. Applied ac frequency range: 0.1 Hz to 100 kHz in (A); scan rate: 100 mV s^{-1} in (B).

Electrochemical impedance spectroscopy (EIS) can reflect the impedance changes of the electrode surface during the modification process. The EIS curve consists of a semicircular part and a linear part. The semicircular part at higher frequencies corresponds to the electron-transfer-limited process and its diameter is equal to the electron transfer resistance (R_{et}). Meanwhile, the linear part at lower frequencies corresponds to the diffusion process. As shown in Fig. 2A, the CuO nanoparticles (curve b) and the graphene-CuO nanocomposites (curve c) modified GCEs exhibit a quite large and a

rather small semicircle diameters of EIS, respectively, as compared with no semicircle at the bare GCE (curve a). The impedance changes in the modification process indicate that CuO nanoparticles and graphene-CuO nanocomposites have been attached to the electrode surface. The quite large R_{et} (1659 Ω) of CuO/Nafion/GCE (curve b) suggests that CuO nanoparticles extremely blocked the electron transfer of probe molecules at electrode surface. The R_{et} of the graphene-CuO/Nafion/GCE (curve c) was estimated to be 193Ω which is much smaller than the Cu-CNTs-Nf electrode [29]. The smaller (EIS) value indicates that the graphene facilitate the electron transportation at electrode surface due to its high conductivity. This confirms that CuO nanograins are uniform and well-separated on the graphene surface and that the graphene acts as an excellent electronic substrate to contribute to much larger response surface and more electron transfer passages. Therefore, the graphene-CuO/Nafion/GCE has higher electrochemical activity than the CuO/Nafion/GCE.

Fig. 2B shows the CVs of bare GCE, CuO/Nafion/GCE and graphene-CuO/Nafion/GCE in 0.1 M KCl electrolyte solution containing 0.01 M $Fe(CN)_6^{4-/3-}$. Compared with the bare GCE (curve a) and CuO/Nafion/GCE (curve b), the graphene-CuO/Nafion/GCE (curve c) displayed much larger peak currents apparently, which further demonstrates that graphene-CuO nanocomposites have a larger electroactive surface than the CuO nanoparticles and can act as a promoter to enhance the electrochemical reaction.

3.3. Electrocatalysis oxidation of glucose at the graphene-CuO/Nafion/GCE
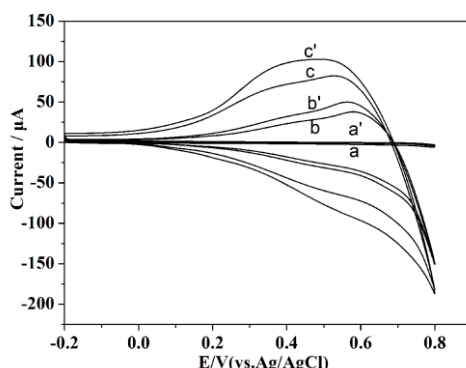
Figure 3. CVs of (a and a') bare GCE, (b and b') CuO/Nafion/GCE and (c and c') graphene-CuO/Nafion/GCE in 0.02 M NaOH in the absence (a, b and c) and presence (a', b' and c') of 1mM glucose, respectively at 50 mV s^{-1}.

The electrocatalytic activity of graphene-CuO nanocomposites towards the oxidation of glucose was examined in 0.02 M NaOH solution. It is found that not only the graphene-CuO nanocomposites but also the CuO nanoparticles could electrochemically catalyze the oxidation of glucose. Furthermore, a better electrocatalytic performance could be exhibited at the graphene-CuO/Nafion/GCE (c,c') than at the CuO/Nafion/GCE (b,b') although not at all at bare GCE (a,a'), which can be seen in Fig 3. Thus, it is suggested that it was at the surface of CuO nanostructures that the electrocatalytic oxidation of glucose occurred and that the graphene just facilitated the catalytic process further. The enhanced performance may be due to the large specific surface area, good

crystallinity, and efficient transport properties of graphene-CuO nanocomposites. Firstly, the uniform and ultra-tiny CuO nanograins highly dispersed on the surface of graphene could contribute to a much larger specific surface area than the CuO nanoparticles tending to aggregate into nanoclusters. Thus, a much larger amount of adsorption sites for glucose could be obtained at the surface of the former than at that of the latter. Secondly, the good crystallinity of CuO nanograins not only improved glucose adsorption but also greatly enhanced glucose activation and the rate of being activated. Thirdly, as an excellent electronic substrate, the graphene could promptly and swiftly transport electrons from CuO nanograins well separated on itself upon the oxidation occurring. The efficient transport property of graphene-CuO nanocomposites was also testified by EIS.

3.4. Effect of potential on amperometric response at the graphene-CuO/Nafion/GCE
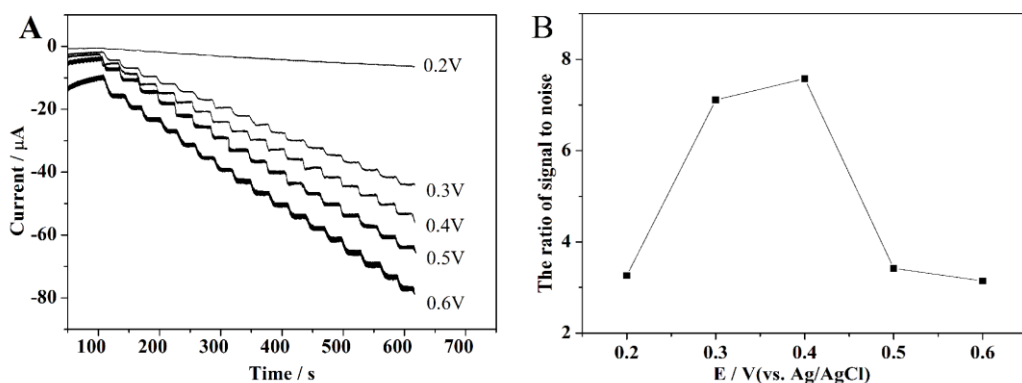
Figure 4. (A) Amperometric response of graphene-CuO/Nafion/GCE with successive addition of 5.0 mL 1 mM glucose to 0.02 M NaOH at different applied potentials (from 0.20 V to 0.60 V); (B) Effect of applied potential on the ratio of signal to noise in the presence of 0.1 M glucose in 0.02 M NaOH solution.

Fig. 4A shows the *I-t* curves of the graphene-CuO/Nafion/GCE in 0.02 M NaOH solution with successive addition of 1 mM glucose at applied potentials from 0.20 to 0.60 V. In the range of 0.20-0.60V, the electrocatalytic oxidation current of glucose increases with the increasing potential. As the potential increasing further, the side reaction takes place on the electrode, which results in the increase of background current and inhibition of glucose oxidation. Notably, the ratio of response current to background current, namely the ratio of signal to noise, increases first and then decreases and the maximum ratio occurs at 0.40 V (Fig, 4B). Thus, an applied potential of 0.40V was chosen as the working potential for further amperometric investigation. Basically, this working potential is less positive than the reported before, demonstrating a greater electrocatalytic ability of the graphene-CuO nanocomposites. This could be ascribed to good crystallinity and well-separated distribution of CuO nanograins as well as high conductivity of graphene.

3.5. Amperometric measurement of glucose
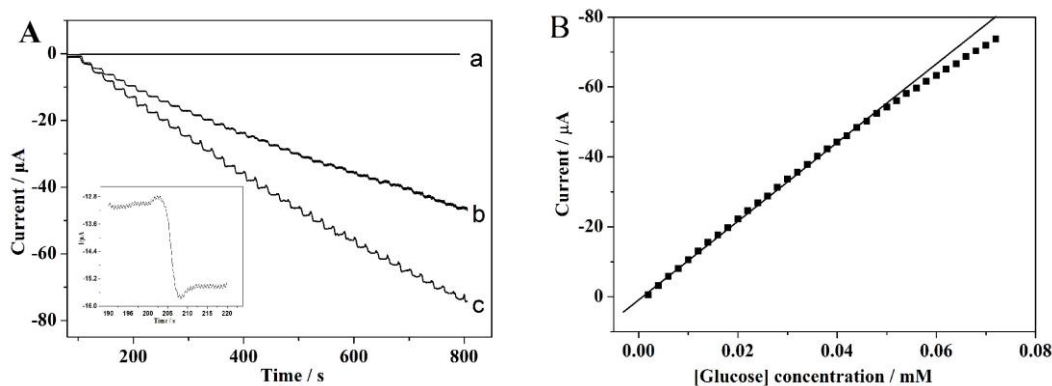
Figure 5. (A) Amperometric response of (a) bare GCE and (b) CuO/Nafion/GCE and (c) graphene-CuO/Nafion/GCE at 0.40 V upon successive addition of 10 µL 1.0 mM glucose to 5.0 mL 0.02 M NaOH solution. The lower left inset is the magnified amperometric response curves of one step addition of curve c; (B) The calibration curve of oxidation currents vs. concentrations of glucose at the graphene-CuO/Nafion/GCE.

Table 1 Comparison of the present graphene-CuO/Nafion/GCE with other nonenzymatic glucose sensor

Electrode	Detection potential	Sensitivity ($\mu A\ mM^{-1}\ cm^{-2}$)	Linear range (mM)	Detection limit (µM)	Reference
Cu_2O/Carbon Vulcan XC-72	-	629	Up to 6	2.4	[10]
Cu/graphene	+0.5	-	Up to 4.5	0.5	[14]
Flower-shaped CuO	+0.58	47.19	0.01-10	1.37	[15]
CuO/graphene	+0.6	1065	0.001-8	1	[21]
Cu-MWCNTs	+0.55	1096	Up to 7.5	1.0	[30]
CuO-NFs	+0.4	431.3	0.006-2.5	0.8	[31]
CuO/TiO_2	+0.7	1321	0.001-2	0.39	[32]
Cu_2O@CRG electrode	+0.45	-	0.1-1.1	1.2	[33]
Pt-AuNCs/SWCNTs	-	-	0.5-45	100	[34]
Graphene-CuO	+0.4	1480	0.002-0.06	0.29	Current work

Fig. 5A shows *I-t* curves of glucose in alkaline solution at the bare GCE, the CuO/Nafion/GCE and the graphene-CuO/Nafion/GCE. With the addition of glucose, no current response is observed at the bare GCE at 0.40V (curve a) and a small amperometric response is observed at CuO/Nafion/GCE (curve b). However, a large, well-defined, amperometric response can be observed at the graphene-CuO/Nafion/GCE (curve c) at 0.40V with successive addition of glucose into 0.02 M NaOH at 20 s interval. The lower left inset of Fig. 5A shows the magnified I-t curves of one step addition of glucose in Fig. 5A (curve c) and clearly displays the response of the graphene-CuO/Nafion/GCE after the

addition of glucose. The electrode responded immediately after glucose was added and the time to achieve 95% steady-state current is no more than 3s, indicating an extraordinarily rapid and sensitive response to glucose. The calibration curve for the graphene-CuO is shown in the Fig. 5B. The current response of the sensor exhibits a linear dependence on the concentration of glucose: I (μA) = -1.023-1045.038 [glucose] (mM), R=0.998. The sensor displays a liner range from 2.0 μM to 0.06 mM, with a sensitivity of 1480 μA mM^{-1} cm^{-2}, and a detection limit of 0.29 μM (S/N=3). The sensitivity of the graphene-CuO/Nafion/GCE is obviously higher than other non-enzymatic glucose sensors, which are summarized in Table 1. The excellent performance could be attributed to the uniform quantum size, good crystallinity and well-separated distribution of CuO nanograins and the efficient transport properties of graphene, which effectively increases the electrocatalysis active areas and promotes electron transfer in the oxidation of glucose.

3.6. Anti-interference property, reproducibility and stability of the graphene-CuO/Nafion/GCE
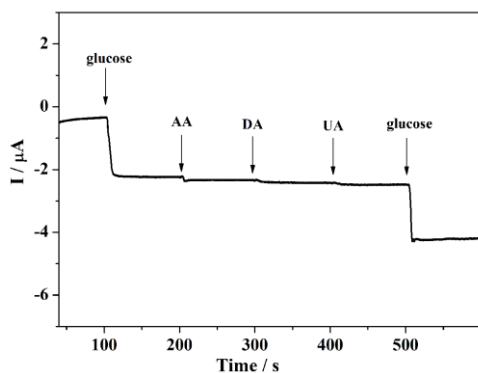
Figure 6. Amperometric responses of graphene-CuO/Nafion/GCE at 0.40V with successive additions of 0.1 mM glucose, 0.1 mM AA, 0.1 mM DA and 0.1 mM UA to 5 mL of 0.02 M NaOH solution.

The poisoning possibility of chloride ions to the activity of graphene-CuO/Nafion/GCE in glucose determination was examined by adding sodium chloride in the supporting electrolyte in measurement. The linear response for glucose at graphene-CuO/Nafion/GCE remains almost constant, demonstrating that the electrode can be used in the presence of chloride ions. Fig. 6. displays the amperometric response to successive additions of 0.1 mM glucose, 0.1mM AA, 0.1mM DA, 0.1mM UA and 0.1 mM glucose in 0.02 M NaOH solution. The current response produced by glucose is far higher than the same concentration of AA, DA, and UA, which implies a good selectivity to the determination of glucose. The responses obtained at the modified electrode to 0.1mM AA, 0.1mM DA, 0.1mM UA are only 8.23%, 4.21% and 0.16% of the response to 0.1mM glucose, respectively. The experimental results indicate that these substances have no obvious interference to the glucose determination, suggesting that the proposed biosensor possesses potential application for the determination of glucose in real samples.

The reproducibility and stability of the developed sensor were further determined. The relative standard deviation (R.S.D) for detection of 0.1 mM glucose with six different sensors prepared under the same conditions was 3.6%, confirming that the preparation method was highly reproducible. Meanwhile, the R.S.D of the sensor response to 0.1 mM glucose was 2.8% for ten successive measurements, indicating that the sensor was very stable. The long-term stability of the sensor was also evaluated by measuring its current response to glucose within a 30-day period. The sensor was exposed to air and its sensitivity was tested every 2 days. The current response of the graphene-CuO/Nafion/GCE was approximately 92% of its original counterpart, which could be mainly attributed to the chemical stability of CuO in basic solution.

4. CONCLUSIONS

A novel electrode material, graphene-CuO nanocomposites, was first synthesized on the template of graphene by a one-step chemical synthesis approach. The graphene-CuO nanocomposites could be used to fabricate an amperometric enzyme-free glucose sensor. The sensor exhibited a high sensitivity, fast response, good stability and low detection limit in response to glucose. The excellent performance can be ascribed to the uniform quantum size and good crystallinity of CuO nanograins, as well as the graphene acting as the synthetic template to highly disperse CuO nanograins on it and as the excellent electronic substrate to efficiently transport electrons. These experimental results demonstrate that graphene-CuO nanocomposites are an attractive material for the fabrication of efficient amperometric sensor.

References

1. S.R. Lee, Y.T. Lee, K. Sawada, H. Takao, M. Ishida, *Biosens. Bioelectron.* 24 (2008) 410.
2. S. Vaddiraju, I. Tomazos, D.J. Burgess, F.C. Jain, F. Papadimitrakopoulos, *Biosens. Bioelectron.* 25 (2010) 1553.
3. J.D. Newman, A.P.F. Turner, *Biosens. Bioelectron.* 20 (2005) 2435.
4. L.H. Li, W.D. Zhang, *Microchim. Acta.* 163 (2008) 305.
5. Y. Li, Y.Y. Song, C. Yang, X.H. Xia, *Electrochem. Commun.* 9 (2007) 981.
6. A. Gutes, C. Carraro, R. Maboudian, *Electrochim. Acta* 56 (2011) 5855.
7. F. Sun, L. Li, P. Liu, Y.F. Lian, *Electroanalysis* 23 (2011) 395.
8. Y.P. Sun, H. Buck, T.E. Mallouk, *Anal. Chem.* 73 (2001) 1599.
9. A. Habrioux, K. Servat, S. Tingry, K.B. Kokoh, *Electrochem. Commun.* 11 (2009) 111.

10. K.M. El Khatib, R.M. Abdel Hameed, *Biosens. Bioelectron*. 26 (2011) 3542.
11. Y. Jiang, S. Decker, C. Mohs, K.J. Klabunde, *J. Catal.* 180 (1998) 24.
12. M. Devaraj, R.K. Deivasigamani, S. Jeyadevan, *Colloids Surf. B: Biointerfaces* 102 (2013) 554.
13. B.J. Wang, L.Q. Luo, Y.P. Ding, D.S. Zhang, Q.L. Zhang, *Colloids Surf. B: Biointerfaces* 97 (2012) 51
14. J. Luo, S.S. Jiang, H.Y. Zhang, J.Q. Jiang, X.Y. Liu, *Anal. Chim. Acta* 709 (2012) 47.
15. A. Umar, M.M. Rahman, A.A. Hajry, Y.B. Hahn, *Electrochem. Commun*. 11 (2009) 278.
16. K.S. Novoselov, A.K. Geim, S.V. Morozov, D. Jiang, Y. Zhang, S.V. Dubonos, I.V. Grigorieva, A.A. Firsov, *Science* 306 (2004) 666.
17. M. Pumera, *Chem Record,* 9 (2009) 211.
18. K.S. Novoselov, A.K. Geim, S.V. Morozov, D. Jiang, M.I. Katsnelson, I.V. Grigorieva, S.V. Dubonos, A.A. Firsov, *Nature* 438 (2005) 197.
19. K.Q. Deng, J.H. Zhou, X.F. Li, *Colloids Surf. B: Biointerfaces* 101 (2013) 183.
20. Y. Wang, Y.M. Li, L.H. Tang, J. Lu, J.H. Li, *Electrochem. Commun*. 11 (2009) 889.
21. Y.W. Hsu, T.K. Hsu, C.L. Sun, Y.T. Nien, N.W. Pu, M.D. Ger, *Electrochimica Acta* 82 (2012) 152.
22. N.I. Kovtyukhova, P.J. Ollivier, B.R. Martin, T.E. Mallouk, S.A. Chizhik, E.V. Buzaneva, A.D. Gorchinskiy, *Chem. Mater*. 11 (1999) 771.
23. H.L. Wang, H.S. Casalongue, Y.Y. Liang, H.J. Dai, *J. Am. Chem. Soc*. 132 (2010) 7472.
24. Y.J. Mai, X.L. Wang, J.Y. Xiang, Y.Q. Qiao, D. Zhang, C.D. Gu, J.P. Tu, *Electrochim. Acta* 56 (2011) 2306.
25. M.S. Dresselhaus, G. Dresselhaus, R. Saito, A. Jorio, *Phys. Rep*. 409 (2005) 47.
26. Z.H. Ni, Y.Y. Wang, T. Yu, Z.X. Shen, *Nano Res* 1 (2008) 273.
27. C.S. Shan, H. Tang, T.L. Wong, L.F. He, S.-T. Lee, *Adv. Mater*. 24 (2012) 2491.
28. J.W. Zhu, G.Y. Zeng, F.D. Nie, X.M. Xu, S. Chen, Q.F. Han, X. Wang, *Nanoscale* 2 (2010) 988.
29. X.H. Kang, Z.B. Mai, X.Y. Zou, P.X. Cai, J.Y. Mo, *Anal. Biochem* 363 (2007) 143.
30. J. Yang, W.-D. Zhang, S. Gunasekarana, *Biosens. Bioelectron*. 26 (2010) 279.
31. W. Wang, L.L. Zhang, S.f. Tong, X. Li, W.B. Song, *Biosens. Bioelectron*. 25 (2009) 708.
32. J.S. Chen, L. Xu, R.Q. Xing, J. Song, H.W. Song , D.L. Liu, J. Zhou, *Electrochem. Commun*. 20 (2012) 75.
33. Q. Yong, F.C. Ye, J.P. Xu, Z.G. Le, *Int. J. Electrochem. Sci.* 7 (2012) 10063.
34. X. Zhu, C.L. Li, X.H. Zhu, M.T. Xu, *Int. J. Electrochem. Sci.* 7 (2012) 8522.